

# Morphology Study of Inverted Planar Heterojunction Perovskite Solar Cells in Sequential Deposition

Asmat Nawaz, Ali Koray Erdinc, Burak Gultekin, Muhammad Tayyib, Ceylan Zafer, Kaiying Wang, M. Nadeem Akram

**Abstract**—In this study, a sequential deposition process is used for the fabrication of PEDOT:PSS based inverted planar perovskite solar cell. A small amount of additive deionized water (DI-H<sub>2</sub>O) was added into PbI<sub>2</sub> + Dimethyl formamide (DMF) precursor solution in order to increase the solubility of PbI<sub>2</sub> in DMF, and finally to manipulate the surface morphology of the perovskite films. A morphology transition from needle like structure to hexagonal plates, and then needle-like again has been observed as the DI-H<sub>2</sub>O was added continuously (0.0 wt% to 3.0wt%). The latter one leads to full surface coverage of the perovskite, which is essential for high performance solar cell.

**Keywords**—Charge carrier diffusion lengths, methylammonium lead iodide, precursor composition, perovskite solar cell, sequential deposition.

## I. INTRODUCTION

HIGHLY efficient and low cost solar cells are being relentlessly pursued by the photovoltaic research community [1]. Very recently, organic-inorganic halide perovskite having general formula of ABX<sub>3</sub>; where A = CH<sub>3</sub>NH<sub>3</sub><sup>+</sup>(MA), B = Pb<sup>+2</sup> or Sn<sup>+2</sup> and X = Cl<sup>-</sup>, Br<sup>-</sup>, I<sup>-</sup> [2], have been proposed with the potential of a breakthrough for the third generation solar devices [3]. In 2009, Miyasaka's group firstly reported perovskite sensitizer with TiO<sub>2</sub> mesoporous electrode and liquid electrolyte and the reported efficiency of the cells was 3.8% [4]. After that, liquid electrolyte was gradually replaced with solid electrolyte such as Spiro-OMeTAD or other materials called hole transporting layer [5]. The devices finally flourished into the current form of planar n-i-p or p-i-n heterojunction devices [6]. Xing et al. have measured electron and hole diffusion lengths; L<sub>D</sub><sup>e</sup> = 130 nm and L<sub>D</sub><sup>h</sup> = 110 nm in the perovskite layer. The promising performance reported for the solar cells based on triiodide perovskite (MAPbI<sub>3</sub>) is because of balanced carrier diffusion lengths [7]. Moreover, diffusion length reported for MAPbI<sub>3-x</sub>Cl<sub>x</sub> is more than 1000 nm. Planar heterojunction structures are preferable because there is no need of mesoscopic layer that needs high sintering temperature [8].

Asmat is with the Dep of Micro and Nano Systems Technology, University College South East Norway, Borre 3184 Norway (corresponding author, e-mail: asmat.nawaz@hbv.no).

Kaiying Wang, M. Nadeem Akram and Muhammad Tayyib are with the Dep of Micro and Nano Systems Technology, University College South East Norway, Borre 3184 Norway.

Ali Koray Erdinc, Burak Gultekin, Ceylan Zafer is with the Ege University, Solar Energy Institute, 35100 Bornova, Izmir, Turkey.

## II. BASIC METHODOLOGY

In perovskite solar cell, the perovskite sensitizer layer is sandwiched between electron transport layers (ETLs) and hole transport layers (HTLs). After absorbing the incident photons, carriers are created in the sensitizer layer, which flow through a pathway including ETLs or HTLs, interface in between, and finally reaching the electrodes for collection [9]. We have fabricated inverted planar structure ITO/PEDOT:PSS/MAPbI<sub>3</sub>/PCBM/Al based solar cell by sequential deposition process. It is very difficult to achieve full surface coverage of perovskite film on an organic layer via single spin coating that crystallizes very quickly especially in DMF. PbI<sub>2</sub> is less polar as compared to the perovskite so it can form a uniform film on the PEDOT:PSS surface. This is the reason why a two-step method is more appropriate as compared to the single-step method for the perovskite layer deposition. However, good surface morphology of the perovskite film is one of the most important factor for a good performance of the morphology of the perovskite films. There are lot of additives such as HI [10], device [11]. The concept of additives has also been used to improve HCl [12], 1,8-diiodooctane [13], 5-ammoniumvaleric iodide [14], CHP [15]. In this study, we have used DI- H<sub>2</sub>O [11] as an additive. Our approach was to form a full surface coverage PbI<sub>2</sub> films on PEDOT:PSS substrates via spin coating by adding controlled amount of DI-H<sub>2</sub>O in PbI<sub>2</sub>/ (DMF) to prepare a homogenous precursor solution at room temperature. After that, methyl ammonium iodide (CH<sub>3</sub>NH<sub>3</sub>I) was added by sequential dipping to form the complete perovskite layer. Eventually, complete cells were fabricated and measurements were carried out done to access their photovoltaic performance.

## III. EXPERIMENTAL SECTION

### A. Synthesis of Methylammonium Iodide (MAI)

30 ml and 20 ml of aqua solutions of hydroiodic acid (56%) and methylamine (40%) respectively were mixed into a round bottom flask and continuous stirred it at 0°C for 2 hours. After that, MAI was precipitated by evaporating the solvent under vacuum with rotary evaporator at 50°C for about 30 minutes. Then the precipitates were washed ten times with diethyl ether which changed the color of the product from pale yellow to colorless. After that, the product was recrystallized in ethanol. Finally, colorless crystals were filtered out and dried at 60 °C in vacuum oven for 24 hours.

### B. Device Fabrication

PEDOT:PSS (hole transport layer) was spin coated at 2800 rpm for 30sec on to an etched, cleaned and oxygen plasma treated ITO substrates and then annealed at 120 °C for 20 minutes. 0.8 M  $\text{PbI}_2$ /DMF precursor solutions with additive DI- $\text{H}_2\text{O}$  (0 wt%, 1 wt%, 2 wt%, 3 wt%) were prepared and stirred overnight at 60 °C. To deposit the perovskite film, first layer of  $\text{PbI}_2$ /DMF (1 wt%) was deposited on to PEDOT:PSS layer by spin coating at different rotation speeds (3000-6000 rpm) for 25 sec and immediately (before drying) dipped into MAI/ Isopropyl alcohol (IPA) solution for 2-3 minutes to form a perovskite film. After that perovskite films were rinsed with IPA for removing extra iodide and annealed at 80 °C for 1-2 minutes. PCBM (electron transport layer) was deposited on the surface of the perovskite layer by spin coating at 1500 rpm for 35 sec and annealed at 80 °C for 15 minutes. In order to coat the contact electrode, a 100 nm of Al was evaporated on the PCBM layer. Fig. 1 shows a schematic illustration of the sequential deposition procedure.

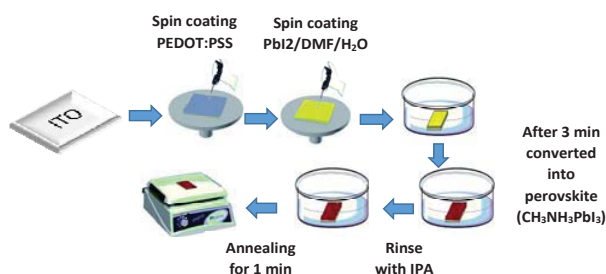


Fig. 1 Schematic illustration of the sequential deposition process

## IV. RESULTS AND DISCUSSIONS

Compact, uniform and void free morphology of the perovskite films are essential for high performance solar cell devices. Additives are used in the precursor solutions to improve the perovskite films morphology [16]. By incorporating additives into the precursor solutions, we can manipulate the crystallization rate of the perovskites [15]. In this study we have used DI- $\text{H}_2\text{O}$  as an additive with different wt%. DMF is a cheap and common solvent for  $\text{PbI}_2$ . To get uniform film by spin coating, 0.8 M  $\text{PbI}_2$ /DMF solution was prepared and heated at 80 °C for 15 min.  $\text{PbI}_2$  has less solubility and results in a colloidal suspension as compared to the homogenous precursor. However, when a controlled amount of DI- $\text{H}_2\text{O}$  (1 wt%) was added into the solution, it became homogenous as shown in Fig. 2.

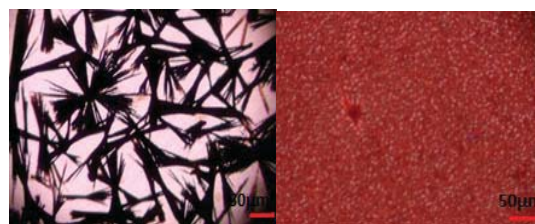
DI- $\text{H}_2\text{O}$  is miscible with DMF, so after adding  $\text{H}_2\text{O}$ , dielectric constant, polarity and solubility parameters of DMF are altered.  $\text{PbI}_2$  is also slightly soluble in  $\text{H}_2\text{O}$  and solubility parameter of  $\text{H}_2\text{O}$ /DMF may be close to that of  $\text{PbI}_2$ . That is why  $\text{PbI}_2$  was completely dissolved when a controlled amount of  $\text{H}_2\text{O}$  was used in the solution [11]. Four different films have been prepared as shown in the optical images in Fig. 3.

The addition of controlled amount of DI- $\text{H}_2\text{O}$  into  $\text{PbI}_2$ /DMF solution helps homogeneous nucleation and crystal

growth because of change in the crystalline morphology of perovskite. Fig. 3 (a) shows optical image of perovskite film when there was no  $\text{H}_2\text{O}$  and it looks like rod shaped crystals. By adding 1 wt%  $\text{H}_2\text{O}$  as shown in Fig. 3 (b) it has been transformed from rod like structure to hexagonal plates crystals [16]. The plate structure morphology of perovskite has produced almost full surface coverage. After adding 2 wt% and 3 wt%  $\text{H}_2\text{O}$  as shown in Figs. 3 (c) and (d) respectively, it has been transformed again from hexagonal plate structure to needle like structure. These results indicate that in order to obtain good and full surface coverage morphology, it is essential that the additive must be used in a controlled amount.

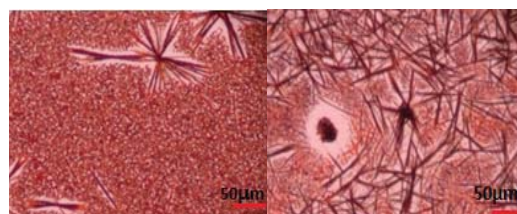


Fig. 2 Photograph of DMF/ $\text{PbI}_2$  precursor solutions consisting of various amounts of additive DI- $\text{H}_2\text{O}$



(a) 0 wt%  $\text{H}_2\text{O}$

(b) 1 wt%  $\text{H}_2\text{O}$



(c) 2 wt%  $\text{H}_2\text{O}$

(d) 3 wt%  $\text{H}_2\text{O}$

Fig. 3 Optical images of perovskite films consisting of various amounts of DI- $\text{H}_2\text{O}$  in  $\text{PbI}_2$ /DMF solution (DI- $\text{H}_2\text{O}$  content is wt% ratio vs DMF)

Fig. 4 exhibits the XRD pattern of  $\text{PbI}_2$  and  $\text{CH}_3\text{NH}_3\text{PbI}_3$  films on mesoporous (m)  $\text{TiO}_2$  substrates. From the figure, it can be seen that  $\text{PbI}_2$  film with hexagonal structure shows a strong peak at 12.6°, having preferred (001) orientation [17]. After dipping the  $\text{PbI}_2$  substrates (wet form) into MAI solution,  $\text{MAPbI}_3$  film was obtained [18] and a series of specific diffraction peaks were observed, which are in a good agreement with literature data on the tetragonal  $\text{CH}_3\text{NH}_3\text{PbI}_3$  phase. The peaks are at 14.08°, 28.38° and 31.87° and are allocated as (110), (220) and (310) planes respectively. All the

diffraction peaks of  $\text{PbI}_2$  are fully transformed into  $\text{CH}_3\text{NH}_3\text{PbI}_3$  structure [19].

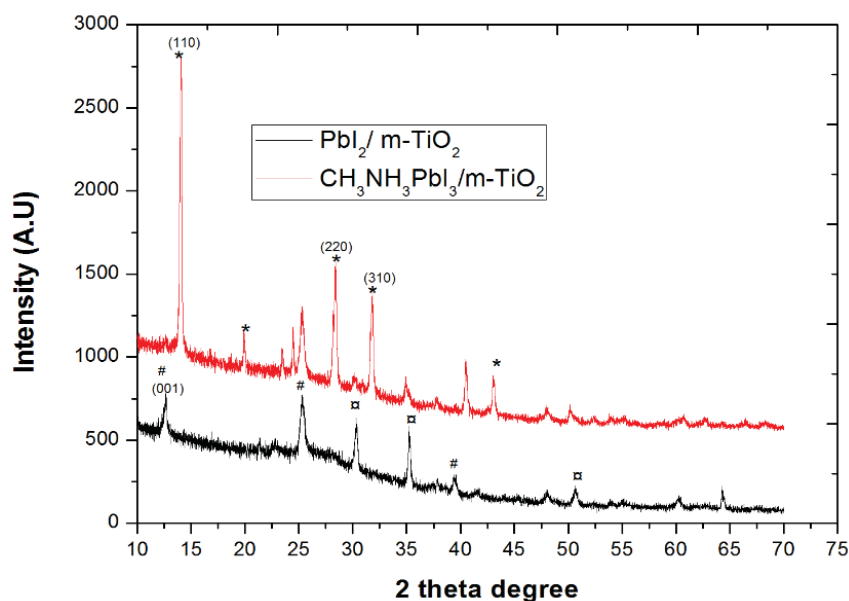


Fig. 4 XRD pattern of  $\text{PbI}_2$  (black) and  $\text{CH}_3\text{NH}_3\text{PbI}_3$  (red) films. The major peaks are from  $\text{PbI}_2$  (#),  $\text{CH}_3\text{NH}_3\text{PbI}_3$  (\*) and FTO/ $\text{mTiO}_2$  substrate. ( $\square$ )

TABLE I  
SUMMARY OF MEASURED PHOTOVOLTAIC PARAMETERS OF PSCs W.R.T THICKNESS

PSCs	Thickness(nm)	Open-circuit voltage $V_{oc}$ (V)	Short-circuit current density $J_{sc}$ ( $\text{mAcm}^{-2}$ )	Fill factor FF	Photon conversion efficiency PCE%
Cell 1	450	0.74	9.43	0.382	2.66
Cell 2	550	0.72	6.09	0.334	1.46
Cell 3	600	0.68	5.60	0.318	1.21
Cell 4	650	0.48	5.44	0.279	0.73

Photovoltaic performance of all the devices were determined under AM 1.5G illumination as shown in Fig. 5 and summarized in Table I.

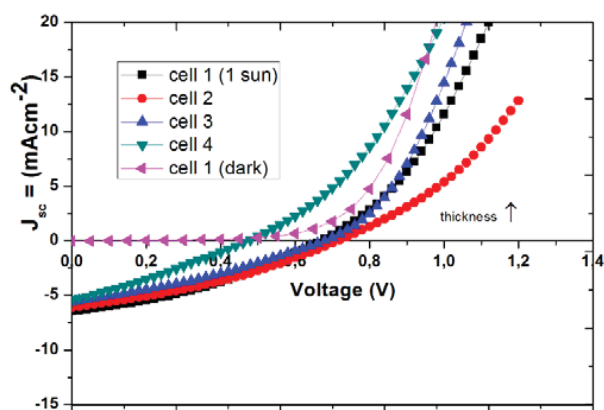


Fig. 5 J-V measurements of different cells w.r.t thickness (perovskite film consist of 1wt% DI-H<sub>2</sub>O)

The thickness of the perovskite absorber layer is a key variable for the performance of such devices. If the perovskite

absorber layer is very thin, then less amount of photons is absorbed, resulting in low photocurrent. However, if perovskite absorber layer is too thick, then the efficiency of the charge carrier extraction is low and carrier recombination becomes dominant. Devices based on mesoporous structure partially avoid this issue by providing the large  $\text{TiO}_2/\text{MAPbI}_3$  interfacial surface area. However, in the planar heterojunction devices the situation becomes more problematic if the absorber layer thickness is higher than the carrier diffusion length. Recent studies have shown that in planar structure the perovskite film thickness from 400nm-800nm can be used for the fabrication of high performance devices which consist of  $\text{MAPbI}_{3-x}\text{Cl}_x$  for both inverted and conventional architectures [20]. Snaith et al. have showed that both holes and electrons have very long diffusion length ( $\sim 1 \mu\text{m}$ ) for mixed halide perovskite ( $\text{MAPbI}_{3-x}\text{Cl}_x$ ), which is much larger than the absorption depth (100-200nm) of the perovskite material [21]. However, this is not true in the case of the parent perovskite ( $\text{MAPbI}_3$ ) material. Xing et al. showed the balanced hole and electron diffusion length of at-least 100 nm for the parent perovskite [7], which is too shorter with respect to the absorption depth of this material. Hence, photo generated

charge carrier in the thicker films cannot be efficiently extracted before recombining [21]. Previous studies based on planar triiodide structure have utilized perovskite layer thickness in the range of 100nm-350 nm [21], [22]. Liu et al showed that the devices consist of both thinnest  $\leq 100$  nm and thickest  $> 400$  nm perovskite ( $\text{MAPbI}_3$ ) films having efficiency of 1-3% [20].

Fig. 5 shows the photovoltaic performance of the four devices with respect to the thickness, and extracted values are summarized in Table I. The devices were fabricated via two-step deposition method. In all the cases, the thickness of the perovskite layer was found to be approximately double of the thickness of the  $\text{PbI}_2$  as shown in Fig. 6, keeping a good match with the previous reports [23], [20].

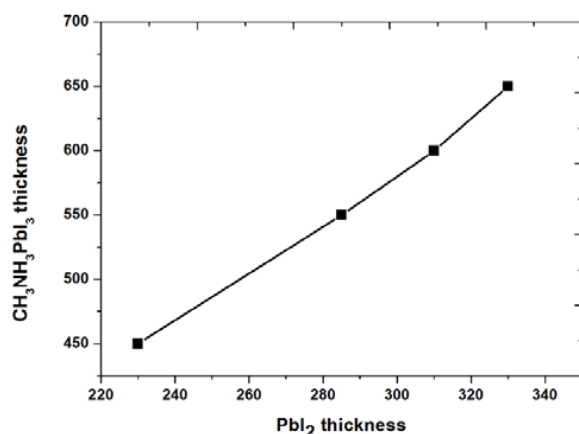


Fig. 6  $\text{CH}_3\text{NH}_3\text{PbI}_3$  thickness vs  $\text{PbI}_2$  thickness, determined by profilometer (thickness units are nanometer)

As summarized in Table I,  $V_{oc}$ ,  $J_{sc}$ , FF and PCE decreases with increase in the thickness of the perovskite layer. The devices with perovskite thickness  $\geq 450$  nm, the deterioration in the device performance is evident. The cause of adverse drop in the PCE of the films having thickness  $\geq 450$  nm, is due to the mismatch between the carrier diffusion length and the perovskite absorption depth. The hole and electron diffusion length for triiodide perovskite have been reported  $\sim 100$  nm. However, for the devices consist of thickest films, there is a significant increase in the recombination of carriers near the center of the film before reaching towards the electrodes for collection [20]. In this study, a two-step method was used for the deposition of perovskite layer. The second step of sequential deposition method was dipping of the film in MAI/IPA solution. The purified IPA contains a small amount of water and PEDOT:PSS can easily dissolve in water. If water penetrates to PEDOT:PSS layer, this can cause defects in the layer. For this reason, sequential deposition method was not implemented previously with PEDOT:PSS based inverted PSC until this study. The main reason of low cell efficiency is may be due to the penetration of IPA/water from pin holes of  $\text{PbI}_2$  layer to the PEDOT:PSS layer. Insufficient purified IPA induced undesirable perovskite morphology. This peculiar situation is shown in Fig. 3 (b). A good surface morphology of

the perovskite film is one of the most important factor for a good performance of the final device. White dots in the figure represent semi-permeable crystal cavities. An ideal surface must not include these cavities to get best efficiency.

## V. SUMMARY AND CONCLUSION

In summary, we have fabricated perovskite planar heterojunction solar cell by sequential deposition method with different thickness of the perovskite film. By increasing the thickness of the parent perovskite ( $\text{MAPbI}_3$ ), there is a significant decrease in the photovoltaic performance of the device. This is due to increased charge recombination near the center of the film. We reported a two-step method for the deposition of perovskite layer. Initially,  $\text{PbI}_2$  was deposited by spin-coating method, and subsequently for the perovskite formation, a dipping process was used. Sequential deposition approach is effective to achieve full surface coverage of the perovskite film, which is essential for high performance devices. For the triiodide perovskites, this approach is not good because the charge diffusion length is too short as compared to the film thickness. That is why there is a need to tailor the thickness of  $\text{PbI}_2$ . A controlled amount of water content (1 wt%) in the  $\text{PbI}_2/\text{DMF}$  solution has exhibited a good impact on the homogeneity of the precursor solution as well as on the morphology of the perovskite films. The smoothness and almost full surface coverage of the perovskite films with 1 wt%  $\text{H}_2\text{O}$  suggests that  $\text{H}_2\text{O}$  can help to achieve homogeneous nucleation by modifying the PEDOT:PSS/ $\text{MAPbI}_3$  interfacial energy.

## ACKNOWLEDGMENTS

The project is funded by KD PhD scholarship, PhD Nano Network grant and NorFab grant. We acknowledge the support of Ege University Solar Energy institute labs.

## REFERENCES

- [1] Z. Xiao, C. Bi, Y. Shao, Q. Dong, Q. Wang, Y. Yuan, *et al.*, "Efficient, high yield perovskite photovoltaic devices grown by interdiffusion of solution-processed precursor stacking layers," *Energy & Environmental Science*, vol. 7, pp. 2619-2623, 2014.
- [2] L. Zheng, Y. Ma, S. Chu, S. Wang, B. Qu, L. Xiao, *et al.*, "Improved light absorption and charge transport for perovskite solar cells with rough interfaces by sequential deposition," *Nanoscale*, vol. 6, pp. 8171-8176, 2014.
- [3] N. J. Jeon, J. H. Noh, Y. C. Kim, W. S. Yang, S. Ryu, and S. I. Seok, "Solvent engineering for high-performance inorganic-organic hybrid perovskite solar cells," *Nat Mater*, vol. 13, pp. 897-903, 2014.
- [4] A. Kojima, K. Teshima, Y. Shirai, and T. Miyasaka, "Organometal halide perovskites as visible-light sensitizers for photovoltaic cells," *J Am Chem Soc*, vol. 131, pp. 6050-1, 2009.
- [5] M. Liu, M. B. Johnston, and H. J. Snaith, "Efficient planar heterojunction perovskite solar cells by vapour deposition," *Nature*, vol. 501, pp. 395-398, 2013.
- [6] L. Meng, J. You, T.-F. Guo, and Y. Yang, "Recent Advances in the Inverted Planar Structure of Perovskite Solar Cells," *Accounts of Chemical Research*, vol. 49, pp. 155-165, 2016.
- [7] G. Xing, N. Mathews, S. Sun, S. S. Lim, Y. M. Lam, M. Grätzel, *et al.*, "Long-Range Balanced Electron- and Hole-Transport Lengths in Organic-Inorganic  $\text{CH}_3\text{NH}_3\text{PbI}_3$ ," *Science*, vol. 342, pp. 344-347, 2013.
- [8] L. Hu, J. Peng, W. Wang, Z. Xia, J. Yuan, J. Lu, *et al.*, "Sequential Deposition of  $\text{CH}_3\text{NH}_3\text{PbI}_3$  on Planar  $\text{NiO}$  Film for Efficient Planar Perovskite Solar Cells," *ACS Photonics*, vol. 1, pp. 547-553, 2014.



- [9] H. Zhou, Q. Chen, G. Li, S. Luo, T.-b. Song, H.-S. Duan, *et al.*, "Interface engineering of highly efficient perovskite solar cells," *Science*, vol. 345, pp. 542-546, 2014.
- [10] G. E. Eperon, S. D. Stranks, C. Menelaou, M. B. Johnston, L. M. Herz, and H. J. Snaith, "Formamidinium lead trihalide: a broadly tunable perovskite for efficient planar heterojunction solar cells," *Energy & Environmental Science*, vol. 7, pp. 982-988, 2014.
- [11] C.-G. Wu, C.-H. Chiang, Z.-L. Tseng, M. K. Nazeeruddin, A. Hagfeldt, and M. Gratzel, "High efficiency stable inverted perovskite solar cells without current hysteresis," *Energy & Environmental Science*, vol. 8, pp. 2725-2733, 2015.
- [12] L. Yang, J. Wang, and W. W.-F. Leung, "Lead Iodide Thin Film Crystallization Control for High-Performance and Stable Solution-Processed Perovskite Solar Cells," *ACS Applied Materials & Interfaces*, vol. 7, pp. 14614-14619, 2015/07/15 2015.
- [13] P. W. Liang, C. Y. Liao, C. C. Chueh, F. Zuo, S. T. Williams, X. K. Xin, *et al.*, "Additive enhanced crystallization of solution-processed perovskite for highly efficient planar-heterojunction solar cells," *Advanced materials*, vol. 26, pp. 3748-3754, 2014.
- [14] A. Mei, X. Li, L. Liu, Z. Ku, T. Liu, Y. Rong, *et al.*, "A hole-conductor-free, fully printable mesoscopic perovskite solar cell with high stability," *Science*, vol. 345, pp. 295-8, 2014.
- [15] Y.-J. Jeon, S. Lee, R. Kang, J.-E. Kim, J.-S. Yeo, S.-H. Lee, *et al.*, "Planar heterojunction perovskite solar cells with superior reproducibility," *Scientific Reports*, vol. 4, p. 6953, 2014.
- [16] B.-E. Cohen and L. Etgar, "Parameters that control and influence the organo-metal halide perovskite crystallization and morphology," *Frontiers of Optoelectronics*, vol. 9, pp. 44-52, 2016.
- [17] P. Luo, Z. Liu, W. Xia, C. Yuan, J. Cheng, and Y. Lu, "A simple in situ tubular chemical vapor deposition processing of large-scale efficient perovskite solar cells and the research on their novel roll-over phenomenon in J-V curves," *Journal of Materials Chemistry A*, vol. 3, pp. 12443-12451, 2015.
- [18] C. Jiang, S. L. Lim, W. P. Goh, F. X. Wei, and J. Zhang, "Improvement of CH<sub>3</sub>NH<sub>3</sub>PbI<sub>3</sub> Formation for Efficient and Better Reproducible Mesoscopic Perovskite Solar Cells," *ACS Applied Materials & Interfaces*, vol. 7, pp. 24726-24732, 2015.
- [19] J. Burschka, N. Pellet, S.-J. Moon, R. Humphry-Baker, P. Gao, M. K. Nazeeruddin, *et al.*, "Sequential deposition as a route to high-performance perovskite-sensitized solar cells," *Nature*, vol. 499, pp. 316-319, 2013.
- [20] D. Liu, M. K. Gangishetty, and T. L. Kelly, "Effect of CH<sub>3</sub>NH<sub>3</sub>PbI<sub>3</sub> thickness on device efficiency in planar heterojunction perovskite solar cells," *Journal of Materials Chemistry A*, vol. 2, pp. 19873-19881, 2014.
- [21] S. D. Stranks, G. E. Eperon, G. Grancini, C. Menelaou, M. J. Alcocer, T. Leijtens, *et al.*, "Electron-hole diffusion lengths exceeding 1 micrometer in an organometal trihalide perovskite absorber," *Science*, vol. 342, pp. 341-4, 2013.
- [22] Q. Chen, H. Zhou, Z. Hong, S. Luo, H.-S. Duan, H.-H. Wang, *et al.*, "Planar Heterojunction Perovskite Solar Cells via Vapor-Assisted Solution Process," *Journal of the American Chemical Society*, vol. 136, pp. 622-625, 2014.
- [23] W. Yan, Y. Li, Y. Li, S. Ye, Z. Liu, S. Wang, *et al.*, "Stable high-performance hybrid perovskite solar cells with ultrathin polythiophene as hole-transporting layer," *Nano Research*, vol. 8, pp. 2474-2480, 2015.